

Isotope constraints on seasonal dynamics of nitrogen in Zhanjiang Bay, a typical mariculture bay in South China

Chunqing Chen^{1, 2}, Qibin Lao^{1, 2}, Fajin Chen^{1, 2, 3, 4*}, Guangzhe Jin^{1, 3, 4}, Jiacheng Li¹, Qingmei Zhu^{1, 3, 4}

¹ College of Ocean and Meteorology, Guangdong Ocean University, Zhanjiang 524088, China

² School of Chemistry and Environment, Guangdong Ocean University, Zhanjiang 524088, China

³ Key Laboratory for Coastal Ocean Variation and Disaster Prediction, Guangdong Ocean University, Zhanjiang 524088, China

⁴ Key Laboratory of Climate, Resources and Environment in Continental Shelf Sea and Deep Sea of Department of Education of Guangdong Province, Guangdong Ocean University, Zhanjiang 524088, China

Received 25 December 2023; accepted 15 March 2024

© Chinese Society for Oceanography and Springer-Verlag GmbH Germany, part of Springer Nature 2024

Abstract

Eutrophication in coastal waters has been increasing remarkably, severely impacting the water quality in mariculture bays. In this study, we conducted multiple isotopic measurements on suspended particulate nitrogen ($\delta^{15}\text{N-PN}$) and dissolved nitrate ($\delta^{15}\text{N-NO}_3^-$ and $\delta^{18}\text{O-NO}_3^-$) in Zhanjiang Bay, a typical mariculture bay with a high level of eutrophication in South China, to investigate the changes in nitrogen sources and their cycling between the rainy and dry seasons. During the rainy season, the study found no significant relation between $\delta^{15}\text{N-PN}$ and $\delta^{15}\text{N-NO}_3^-$ due to the impact of heavy rainfall and terrestrial erosion. In the upper bay, a slight nitrate loss and slightly higher $\delta^{15}\text{N-NO}_3^-$ and $\delta^{18}\text{O-NO}_3^-$ values were observed, attributed to intense physical sediment-water interactions. Despite some fluctuations, nitrate concentrations in the lower bay mainly aligned with the theoretical mixing line during the rainy season, suggesting that nitrate was primarily influenced by terrestrial erosion and that nitrate isotopes resembled the source. Consequently, the isotopic values of nitrate can be used for source apportionment in the rainy season. The results indicated that soil nitrogen (36%) and manure and sewage (33%) were the predominant nitrogen sources contributing to nitrogen loads during this period. In contrast, the dry season saw a deficient ammonium concentration ($<0.2 \mu\text{mol/L}$) in the bay, due to nearly complete consumption by phytoplankton during the red tide period. Additionally, the significant loss of nitrate and simultaneous increase in the stable isotopes of dissolved and particulate nitrogen suggest a strong coupling of assimilation and mineralization during the dry season. More active biogeochemical processes during the dry season may be related to decreased runoff and increased water retention time. Overall, our study illustrated the major seasonal nitrogen sources and their dynamics in Zhanjiang Bay, providing valuable insights for formulating effective policies to mitigate eutrophication in mariculture bays.

Key words: nitrogen, stable nitrogen isotopes, biogeochemical processes, eutrophication, Zhanjiang Bay

Citation: Chen Chunqing, Lao Qibin, Chen Fajin, Jin Guangzhe, Li Jiacheng, Zhu Qingmei. 2024. Isotope constraints on seasonal dynamics of nitrogen in Zhanjiang Bay, a typical mariculture bay in South China. *Acta Oceanologica Sinica*, 43(6): 60–70, doi: 10.1007/s13131-024-2373-0

1 Introduction

Coastal waters, situated between the land and ocean, possess rich biological resources and diverse ecosystems that provide invaluable services for the survival and development of humanity (Dai et al., 2023). The behavior of nitrogen (N), a major limiting nutrient for primary production in coastal waters, is complex due to complicated hydrodynamics, various biochemical processes, and human interference that govern the fate of N (Dähnke et al., 2008; Lao et al., 2019; Wankel et al., 2007). In particular, increasing terrestrial N inputs strongly influence the coastal N cycle and environmental health, causing a series of environmental problems, such as eutrophication, seasonal hypoxia, and harmful algal blooms in coastal waters (Dai et al., 2023; Howarth, 2008; Khangaonkar et al., 2018; Lao et al., 2023b). Consequently, mul-

iple N sources and their time-varying nature over recent decades have made it more challenging to understand the fate of N in coastal waters (Ye et al., 2016; Yan et al., 2017).

Among many methods, nitrate dual isotopes ($\delta^{15}\text{N-NO}_3^-$ and $\delta^{18}\text{O-NO}_3^-$) and the nitrogen isotope of particulate N ($\delta^{15}\text{N-PN}$) are powerful tools that have been successfully used to reveal sources and transformation processes of N in marine systems (Chen et al., 2020, 2022a; Lao et al., 2019; Sigman et al., 2005; Ye et al., 2016; Yan et al., 2017). Various N sources can be differentiated based on their isotopic fingerprint features (distinct ranges of isotopic values) (Kendall, 1998; Xue et al., 2009). For example, N sources from sewage and manure are generally characterized by higher $\delta^{15}\text{N}$ values (10‰–20‰) than soil N, fertilizer, and atmospheric deposition (Kendall, 1998; Xue et al., 2009), and the

Foundation item: The National Natural Science Foundation of China under contract Nos 42276047, 92158201 and U1901213; the Entrepreneurship Project of Shantou under contract No. 2021112176541391; the Scientific Research Start-Up Foundation of Shantou University under contract No. NTF20006.

*Corresponding author, E-mail: fjchen@gdou.edu.cn

$\delta^{18}\text{O}$ values from atmospheric deposition (>50‰) are much higher than those from other sources (<25‰) (Chen et al., 2019). Using the isotopic values from different sources, the relative contribution of these sources to seawater can be quantified with Bayesian models to distinguish the main sources of N pollution in the ocean (Chen et al., 2022a; Lao et al., 2019). In addition, stable N isotopes can be used to trace biogeochemical processes because lighter N (^{14}N) is preferentially utilized or transformed during N cycles (Granger et al., 2008; Sigman et al., 2005). Therefore, a better understanding of N sources and cycles in marine systems can be achieved by using stable isotopes of particulate and dissolved N.

Zhanjiang Bay, a typical semi-enclosed bay located in the northwestern South China Sea (SCS), is a renowned maricultural production and export region in China. However, rapid industrialization and urbanization have led to increasing eutrophication stress in the bay (He et al., 2023). This is mainly due to the large influx of terrestrial nutrients and intense local human activity (He et al., 2023; Li et al., 2020). More importantly, intensified human activities, including artificial dams and dredging, have significantly increased the intrusion of seawater from the outer SCS over the past decades. This intrusion can introduce and retain contaminants in the bay (Lao et al., 2022b), thereby exacerbating the eutrophication of seawater in the bay (He et al., 2023). This significantly threatens maricultural breeding activities in Zhanjiang Bay (Lao et al., 2022b). The complexity of the hydrodynamic processes and intense human activity make the dynamic processes of N in the bay more complex. However, a systematic understanding of N sources and their migration and transformation processes in mariculture bays remains limited, which greatly hinders the control of eutrophication and pollution in mariculture bays. To address this issue, the seasonal stable isotopes of dissolved N ($\delta^{15}\text{N}\text{-NO}_3^-$ and $\delta^{18}\text{O}\text{-NO}_3^-$) and particulate N (PN and $\delta^{15}\text{N}\text{-PN}$), along with other chemical properties, were investigated to reveal the variability of N sources and N cycling processes in this semi-enclosed bay.

2 Material and methods

2.1 Study area and field sampling

Zhanjiang Bay, surrounded by the developing coastal city of Zhanjiang in Guangdong Province, South China, has a population of approximately 7.3 million (Chen et al., 2022b). The bay spans an area of about 490 km², with depths ranging from 2 m in the upper bay to 32 m in the lower bay (Fig. 1). Zhanjiang Bay is geographically and hydrodynamically complex, mainly influenced by the local discharge from the Suixi River at the top of the upper bay and the intrusion of high-salinity water from the SCS through a narrow channel at the bay mouth (~2 km wide) (Lao et al., 2022b). Zhanjiang Bay is famous for its mariculture industry, which includes cage culturing and oyster farming. Oyster culture is mainly located in the upper bay, while cage culture is primarily in the lower bay (Chen et al., 2022b). However, due to the influence of intensive human activities and weak hydrodynamic conditions, seawater pollution in the bay, such as eutrophication, is gradually intensifying (He et al., 2023). Affected by the East Asian Monsoon, the annual rainfall in this region is approximately 1 731 mm, with over 85% of the annual rainfall occurring in the rainy season (April to October) and only 15% of the annual rainfall in the dry season (November to March of the following year) (Chen et al., 2019, 2021).

Two cruises were conducted in Zhanjiang Bay, China in

September 2017 and March 2018 (Fig. 1). A total of 26 seawater sampling stations were established from the top of the upper bay to the outer bay during these two periods (Fig. 1). Seawater samples were collected using 10-L Niskin bottles. The temperature, salinity, and depth of the water were determined onsite using an RBR Maestro multiparameter water quality monitor (RBRmaestro3, RBR, Canada). For the collection of Chl-*a*, PN, and $\delta^{15}\text{N}\text{-PN}$ samples, approximately 1 000 mL of seawater was filtered immediately after sampling through precombustion (450°C, 4 h) GF/F (glass fiber filters, 47-mm diameter) and then frozen at -20°C until further analysis. For the samples of nutrients and nitrate dual isotopes ($\delta^{15}\text{N}\text{-NO}_3^-$ and $\delta^{18}\text{O}\text{-NO}_3^-$), the seawater was filtered through a cellulose acetate membrane, and the filtrate was transferred into acid-washed polyethylene bottle and stored at -20°C for laboratory analysis.

2.2 Chemical analyses

Dissolved oxygen (DO) was measured using Winkler titration with a precision of 0.07 mg/L. Chl-*a* samples were extracted using 90% acetone, and the levels were determined using the fluorometric method. Nutrient samples (NO_3^- , NO_2^- , NH_4^+ , PO_4^{3-} , and SiO_3^{2-}) were analyzed using a San++ continuous flow analyzer (Skalar, Netherlands).

The PN and $\delta^{15}\text{N}\text{-PN}$ samples were tightly packed into a tin cup and acidified with concentrated HCl vapor for at least two days to remove carbonate. Subsequently, the HCl was removed in a caustic soda dryer for 48 h (Lao et al., 2023a). The samples were then analyzed using an elemental isotope ratio mass spectrometer (EA Isolink-253 Plus, Thermo Fisher Scientific, USA). Atmospheric N_2 references were utilized for $\delta^{15}\text{N}\text{-PN}$ measurements. The average standard deviation of PN was $\pm 0.1\%$, and the precision for $\delta^{15}\text{N}\text{-PN}$ was $\pm 0.2\%$.

The analysis of $\delta^{15}\text{N}\text{-NO}_3^-$ and $\delta^{18}\text{O}\text{-NO}_3^-$ was conducted using a chemical method (cadmium-azide) (McIlvin and Altabet, 2005). Before determination, the nitrite in the seawater was removed using sulfamic acid (Granger and Sigman, 2009). The nitrate in the sample was then reduced to nitrite by Cd and further reduced to nitrous oxide using sodium azide buffered with acetic acid at pH 4–5. The TraceGas was then used to purify and separate the nitrous oxide, and the compositions of $\delta^{15}\text{N}\text{-NO}_3^-$ and $\delta^{18}\text{O}\text{-NO}_3^-$ were determined by a GasBench II-MAT 253 (MAT 253 Plus, Thermo Scientific, United States). Isotope standard materials, including USGS34 ($\delta^{15}\text{N} = -1.8\%$, $\delta^{18}\text{O} = -27.9\%$), IAEA-NO3 ($\delta^{15}\text{N} = 4.7\%$, $\delta^{18}\text{O} = 25.6\%$), and USGS32 ($\delta^{15}\text{N} = 180\%$, $\delta^{18}\text{O} = 25.7\%$), were used in this study. USGS32 and USGS34 were used to create nitrogen and oxygen isotope standard curves, and IAEA-NO3 was used for quality control monitoring. The reproducibility of duplicates for $\delta^{15}\text{N}\text{-NO}_3^-$ and $\delta^{18}\text{O}\text{-NO}_3^-$ was <0.3‰ and <0.6‰, respectively, with mean differences of $\pm 0.1\%$ and $\pm 0.3\%$, indicating high precision in the measurements.

2.3 Conservative mixing model

In this study, a conservative mixing model was used to calculate the mixing between diluted riverine water and seawater in the bay to reveal the behavior of various N species along the salinity gradient (Fry, 2002; Lao et al., 2019; Ye et al., 2016). The formula is as follows:

$$N_{\text{mix}} = q \times N_{\text{d}} + (1 - q) \times N_{\text{m}}, \quad (1)$$

where N_{d} and N_{m} denote the concentrations of various N species in the diluted water endmember and marine endmember, re-

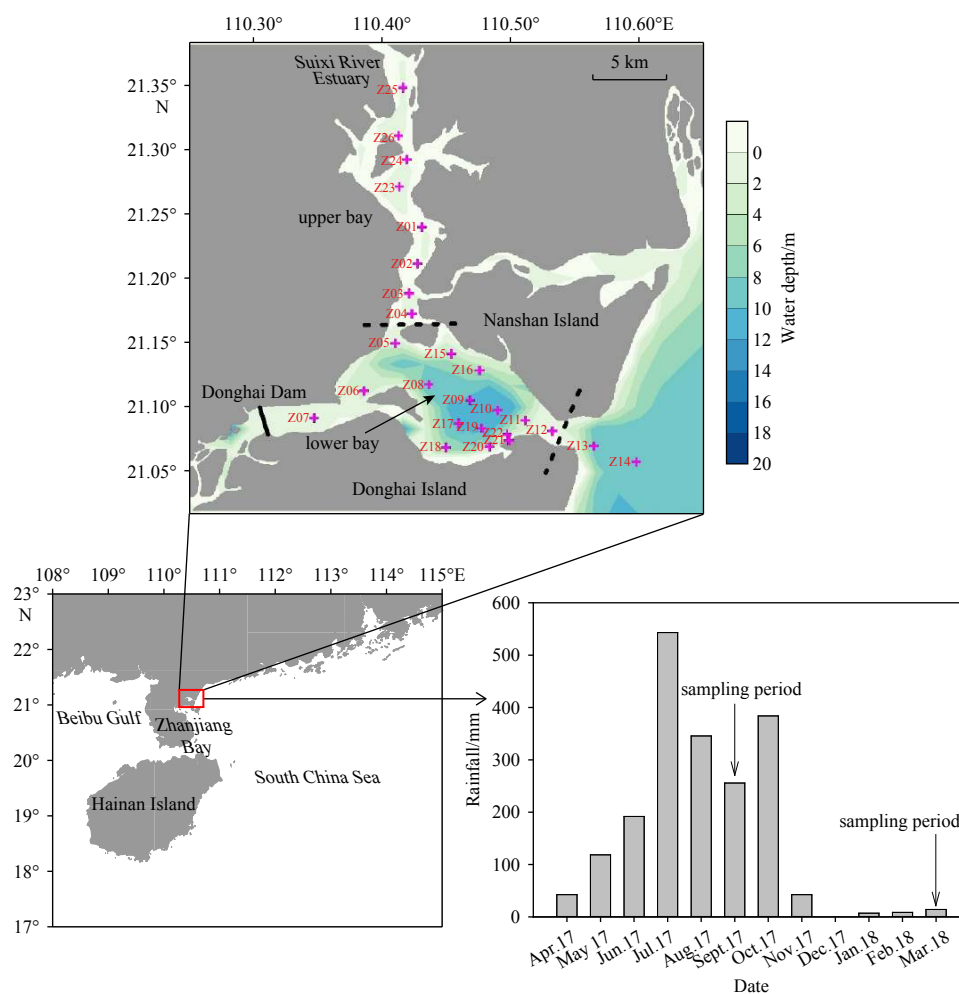


Fig. 1. Study area and the sampling sites in Zhanjiang Bay. The monthly rainfall data from April 2017 to March 2018 in Zhanjiang Bay were obtained from [Chen et al. \(2021\)](#).

spectively, and q denotes the contribution of diluted water to each sample, calculated from salinity as follows:

$$q = (S_m - S_{\text{mix}}) / (S_m - S_d), \quad (2)$$

where S_{mix} , S_d , and S_m denote the salinity of the sample, diluted water end-member, and marine end-member, respectively.

Additionally, the isotopic composition (δ_{mix}) of various N species in a sample is the concentration-weighted mean of values derived from diluted water and marine end-members during physical mixing. The formula is as follows:

$$\delta_{\text{mix}} = [q \times N_d \times \delta_d + (1 - q) \times N_m \times \delta_m] / N_{\text{mix}}, \quad (3)$$

where δ_d and δ_m denote the isotopic values of various N species

in the diluted water and marine end-members, respectively.

In this study, the diluted water end-member was selected from the lowest-salinity water at the top of the upper bay (Station Z25), and the marine end-member was selected from the highest-salinity water in the outer bay (Stations Z13 and Z14). Endmember values are listed in [Table 1](#).

3 Results

3.1 Physicochemical parameters

The seasonal distributions of the physicochemical parameters are illustrated in [Fig. 2](#). Seawater temperature was higher in the rainy season (29.9–32.9 °C) and lower in the dry season (22.2–29.4 °C). Significant variations in salinity were observed in the bay (t -test, $p < 0.01$), with lower values in the rainy season

Table 1. Definitions of the diluted water and marine end-members

	End-member	Salinity	NO ₃ ⁻ concentration/ (μmol·L ⁻¹)	NH ₄ ⁺ concentration/ (μmol·L ⁻¹)	PN concentration/ (mg·L ⁻¹)	δ ¹⁵ N-NO ₃ ⁻ / ‰	δ ¹⁵ N-PN / ‰	δ ¹⁸ O-NO ₃ ⁻ / ‰
September	Diluted water	15.04	47.72	5.82	0.078	7.3	6.8	-0.6
	Marine	27.12	3.96	2.24	0.109	0.5	9.6	4.1
March	Diluted water	20.59	78.11	0.21	0.054	6.1	9.4	6.9
	Marine	29.50	1.48	0.01	0.052	1.4	8.6	11.3

Note: PN: particulate nitrogen.

(15.04–27.89) and higher values in the dry season (20.59–30.46). There was a remarkable salinity gradient from the upper bay to the outer bay, with low salinity occurring at the top of the upper bay, while high salinity was observed in the outer bay during both seasons. The DO values in the rainy season (3.79–7.33 mg/L)

were much lower than those in the dry season (6.99–10.50 mg/L). Low DO values were recorded at the top of the upper layer during the rainy season. However, the Chl-*a* concentration in the rainy season (2.09–22.33 $\mu\text{g/L}$) was remarkably higher than that in the dry season (1.52–11.37 $\mu\text{g/L}$).

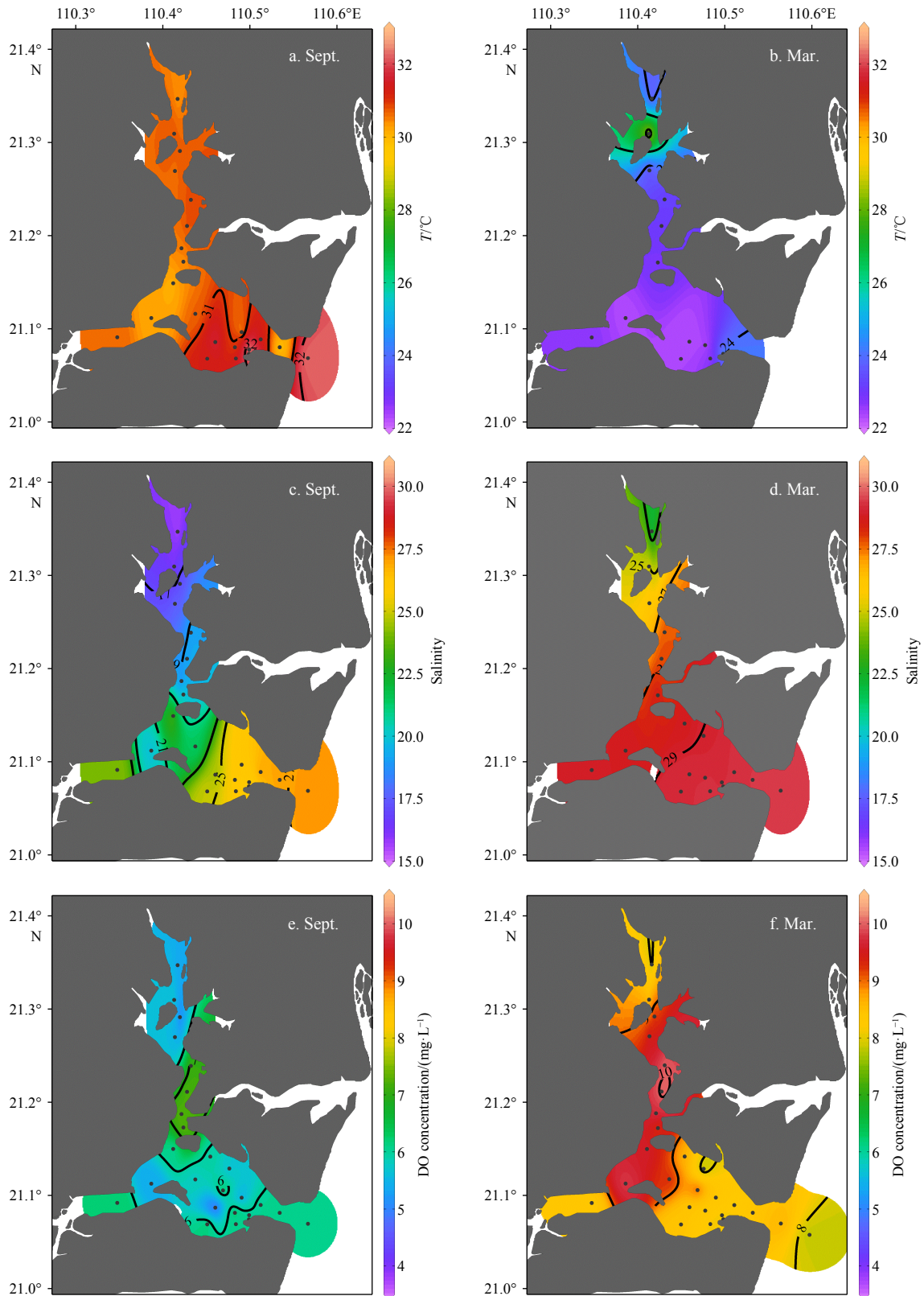


Fig. 2.

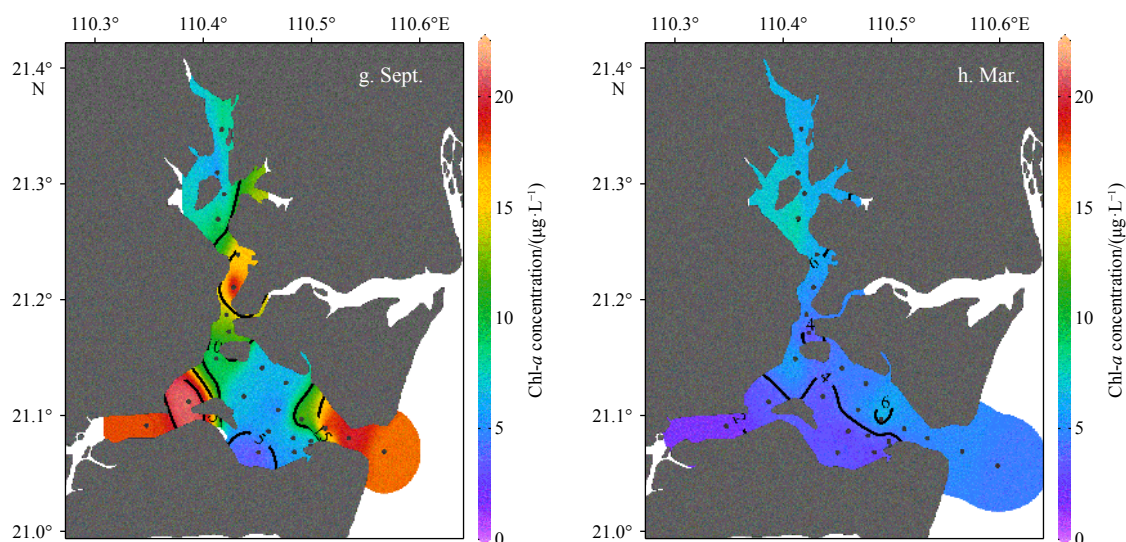


Fig. 2. Spatial distribution of physiochemical parameters (temperature (T), salinity, DO and Chl- a concentrations) in the surface water of Zhanjiang Bay during the rainy (September) and dry (March) seasons.

3.2 Nutrient concentrations

The seasonal distributions of the dissolved nutrients (NO_3^- , NO_2^- , NH_4^+ , PO_4^{3-} , and SiO_3^{2-}) and PN are presented in Fig. 3. They varied significantly between the seasons. Generally, high concentrations of dissolved nutrients were observed in the upper bay, and the concentrations gradually decreased towards the outer bay. The concentrations of dissolved nutrients [$(15.34 \pm 9.60) \mu\text{mol/L}$ for NO_3^- , $(2.87 \pm 1.40) \mu\text{mol/L}$ for NO_2^- , $(5.87 \pm 2.28) \mu\text{mol/L}$ for NH_4^+ , $(4.07 \pm 1.42) \mu\text{mol/L}$ for PO_4^{3-} , and $(20.07 \pm 12.25) \mu\text{mol/L}$ for SiO_3^{2-}] and PN [$(0.075 \pm 0.022) \text{mg/L}$] in the rainy season were higher than those in the dry season [$(6.83 \pm 14.93) \mu\text{mol/L}$ for NO_3^- , $(0.74 \pm 1.21) \mu\text{mol/L}$ for NO_2^- , $(0.03 \pm 0.03) \mu\text{mol/L}$ for NH_4^+ , $(1.28 \pm 0.78) \mu\text{mol/L}$ for PO_4^{3-} , $(4.56 \pm 5.97) \mu\text{mol/L}$ for SiO_3^{2-} , and $(0.057 \pm 0.021) \text{mg/L}$ for PN], which was in agreement with our previous observation in the bay (He et al., 2023), reflecting more terrestrial nutrient discharge in the rainy season. In addition, PN varied similarly to Chl- a during both seasons.

3.3 Isotope compositions

The $\delta^{15}\text{N}-\text{NO}_3^-$ values ranged from 0.5‰ to 7.3‰ in the rainy season and from 1.0‰ to 7.9‰ in the dry season, showing similar ranges between seasons and generally decreasing from the upper bay to the outer bay (Fig. 4). However, the values of $\delta^{15}\text{N}-\text{NO}_3^-$ in the upper bay during the dry season were higher compared to the rainy season (Fig. 4). The $\delta^{18}\text{O}-\text{NO}_3^-$ values ranged from -3.5‰ to 9.1‰ in the rainy season and from -1.4‰ to 18.9‰ in the dry season, with higher values in the dry season (an average of 8.7‰) than in the rainy season (an average of 1.9‰). Unlike the $\delta^{15}\text{N}-\text{NO}_3^-$, the lower $\delta^{18}\text{O}-\text{NO}_3^-$ values occurred in the upper bay, with an increasing trend towards the outer bay (Fig. 4).

The $\delta^{15}\text{N}-\text{PN}$ values in the rainy season (ranging from 3.1‰ to 11.1‰, an average of 5.6‰) were lower than those in the dry season (ranging from 6.5‰ to 11.6‰, an average of 9.2‰). Except for the higher $\delta^{15}\text{N}-\text{PN}$ values in the outer bay during the rainy season, the values generally decreased from the upper bay to the outer bay (Fig. 4). The distinct seasonal and spatial distributions of isotopic values suggest seasonal N sources and biogeochemical processes in the bay.

4 Discussion

4.1 Seasonal nutrient patterns in Zhanjiang Bay

In Zhanjiang Bay, nutrient concentrations in the upper bay were remarkably higher than those in the lower bay during both seasons (Fig. 3), consistent with observations by He et al. (2023) and Li et al. (2020). Similarly, low salinity was recorded in the upper bay (Fig. 2), indicating that elevated nutrient levels were predominantly influenced by terrestrial input. Heavy rainfall in this region typically occurs from April to October (Lao et al., 2022b). Such rainfall can erode and wash away land-based pollutants into the rivers surrounding Zhanjiang Bay, ultimately entering the coastal waters (He et al., 2023). The nutrient concentrations increased significantly during the rainy season, indicating the significant impact of heavy land-based sources discharged from anthropogenic activities (He et al., 2023; Zhang et al., 2021). Over the past decades, increasing terrestrial nutrient inputs have contributed to enhanced eutrophication in the bay (He et al., 2023). However, in the lower bay, the lower nutrient levels could be attributed to the intrusion of high-salinity water from the outer bay. Water mass transport dramatically affects nutrient distribution, thus impacting local marine ecosystems (Lao et al., 2022a, 2023b, 2023c). Human activities have significantly increased the intrusion of high-salinity water from the outer bay over the past two decades (Lao et al., 2022b), resulting in the dilution of nutrients in the lower bay. Although the intrusion of high-salinity water was more pronounced in summer owing to the stronger west-Guangdong coastal current during this period (Lao et al., 2022b), the nutrient concentration in the lower bay during the rainy season was still significantly higher than that during the dry season (t -test, $p < 0.01$) (Fig. 3). This suggests that during the rainy season, terrestrial inputs had a more pronounced effect on nutrient distribution than water mass transportation from the outer bay.

Notably, the N/P ratio in the two seasons (ranging from 4.0 to 11.2, an average of 6.2 in the rainy season, and from 0.7 to 22.6, an average of 5.1 in the dry season) was significantly lower than the Redfield ratio (16.0). High N and P concentrations suggest that N and P did not act as limiting nutrients in the bay and that the environmental conditions were favorable for phytoplankton blooms (Yang et al., 2018). Over recent decades, eutrophication

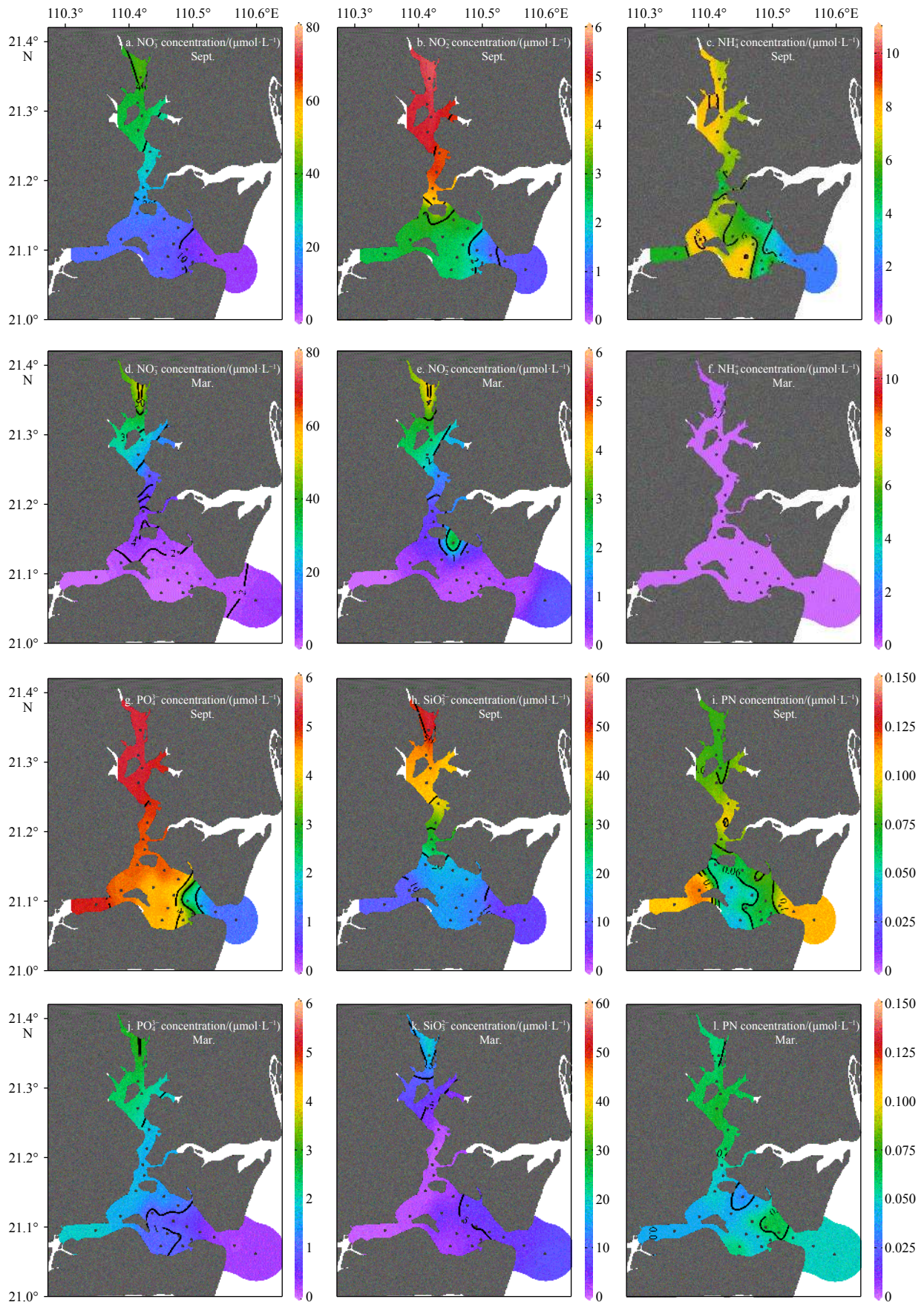


Fig. 3. Spatial distribution of dissolved nutrients (NO_3^- , NO_2^- , NH_4^+ , PO_4^{3-} , and SiO_3^{2-}) and particulate nitrogen (PN) in the surface water of Zhanjiang Bay during the rainy (September) and dry (March) seasons.

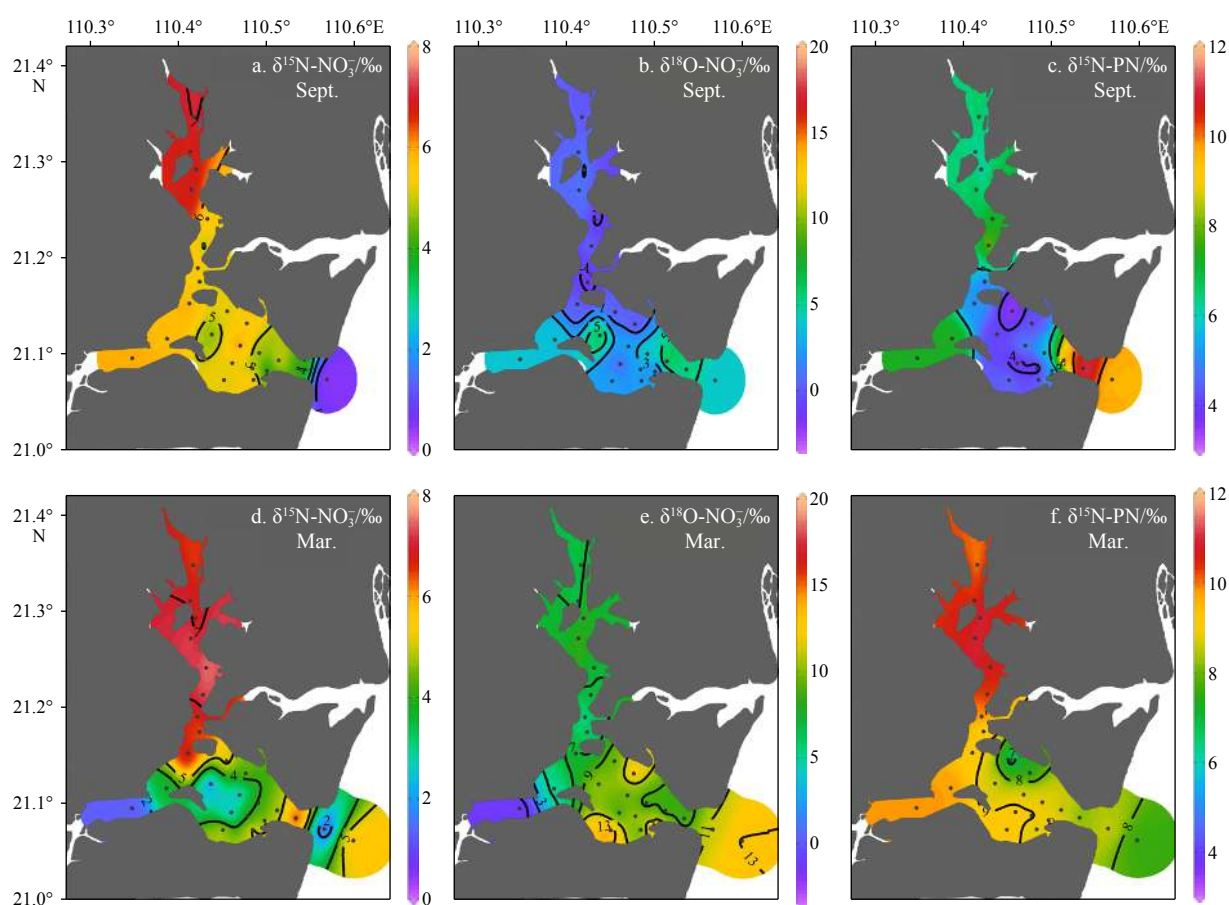


Fig. 4. Spatial distribution of $\delta^{15}\text{N-NO}_3^-$, $\delta^{18}\text{O-NO}_3^-$ and $\delta^{15}\text{N-PN}$ in the surface water of Zhanjiang Bay during the rainy (September) and dry (March) seasons.

and harmful algal blooms have increased substantially in the bay (He et al., 2023; Zhang et al., 2022). Before the 1980s, harmful algal blooms rarely occurred in Zhanjiang Bay, but have occurred periodically and frequently since the 2000s (Zhang et al., 2022). This is mainly due to the increasing nutrient input in the bay, particularly P input (He et al., 2023; Zhang et al., 2022). The dissolved inorganic nitrogen concentration increased threefold from 1990 to 2019, while the P concentration increased 21-fold owing to the continuous input of high-concentration phosphorus from industrial factories around Zhanjiang Bay (He et al., 2023; Zhang et al., 2022). The faster rate of increase in the P concentration in the bay has been responsible for the decrease in the N/P ratio over the past decades (He et al., 2023). Therefore, the ecosystem in Zhanjiang Bay has shifted from P-limited oligotrophic conditions before the 2020s to N-limited eutrophic conditions (Zhang et al., 2022). This implies that the N input plays an important role in the health of the Zhanjiang Bay ecosystem. However, in addition to the impact of the watershed, sewage outlets around Zhanjiang Bay can also input large amounts of anthropogenic nitrogen into the bay (Zhang et al., 2021), resulting in a complex and diversified source of N in the bay.

4.2 Biological processes of N in Zhanjiang Bay

In the rainy season, the negative offset of NO_3^- , along with slightly positive offsets in $\delta^{15}\text{N-NO}_3^-$, and offset- $\delta^{18}\text{O-NO}_3^-$ in the upper bay (areas with lower salinity areas) (Figs 5a and c) indicated the consumption of NO_3^- . The processes of denitrification and phytoplankton assimilation should be ruled out for the NO_3^-

consumption in the upper bay during the rainy season due to the high DO level (>5 mg/L) and decoupling of $\delta^{15}\text{N-NO}_3^-$ and $\delta^{18}\text{O-NO}_3^-$ (Fig. 6c). In addition, a high concentration of NH_4^+ (>5 $\mu\text{mol/L}$) was observed in the upper bay in the rainy season, and phytoplankton preferentially assimilated NH_4^+ under sufficient NH_4^+ conditions (Chen et al., 2022c; Glibert et al., 2016). Therefore, the assimilation of NH_4^+ (rather than NO_3^-), by phytoplankton should be responsible for the negative offset- $\delta^{15}\text{N-PN}$ value, while the positive offset- $\delta^{15}\text{N-NO}_3^-$ values could be influenced by the intense physical sediment-water interaction.

Active NO_3^- consumption induced by denitrification in the sediments results in an efflux of NO_3^- from the upper overlying seawater to the sediments, thereby consuming NO_3^- and enriching $\delta^{15}\text{N-NO}_3^-$ in the water column (Chen et al., 2022c; Ye et al., 2016; Zhang et al., 2013). Indeed, the upper bay is narrow and shallow, and is substantially influenced by tidal pumping. In particular, tidal pumping is stronger in September (Wang et al., 2021), which can promote the bidirectional exchange of materials, including nutrients, between the sediment pore water and the overlying water. This process can increase the $\delta^{15}\text{N-NO}_3^-$ value but lead to the consumption of NO_3^- in seawater due to denitrification-induced enrichment of nitrate isotopes in sediments (Chen et al., 2022c).

Both offset- NO_3^- and offset- $\delta^{15}\text{N-NO}_3^-$ values in the lower bay fluctuated on the theoretical mixing line during the rainy season (Fig. 5), indicating that the NO_3^- is in a conservative mixing state. However, similar to the upper bay, significant positive correlations were found between Chl-*a* and PN in the lower bay during

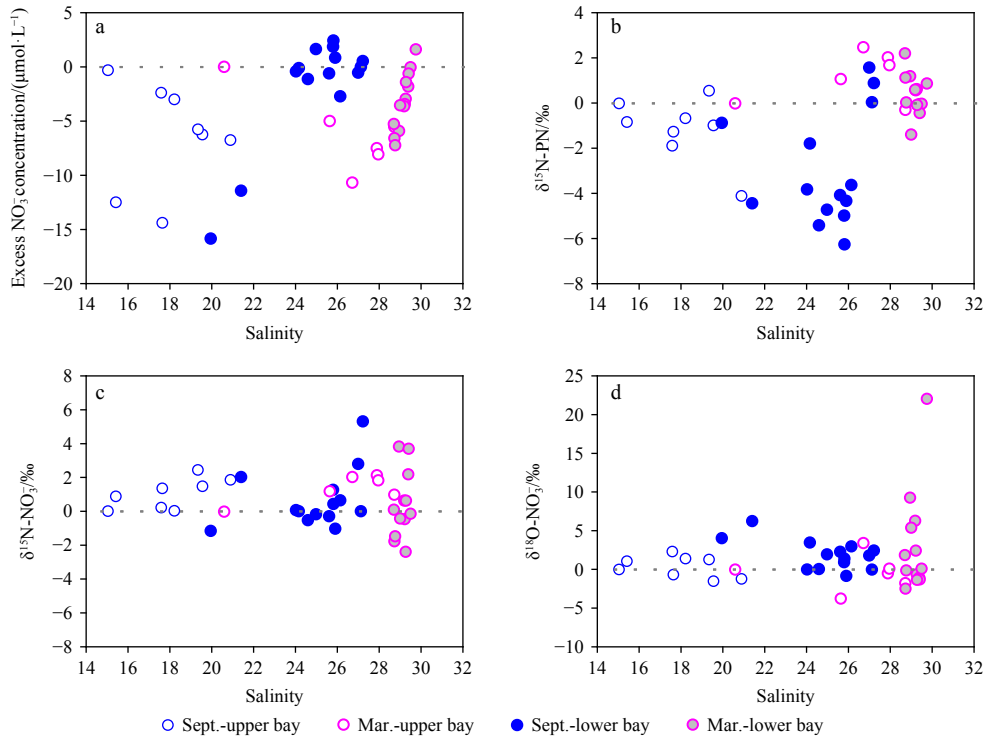


Fig. 5. Distributions of offset excess NO_3^- concentration, $\delta^{15}\text{N-PN}$, $\delta^{15}\text{N-NO}_3^-$, and $\delta^{18}\text{O-NO}_3^-$ along the salinity in Zhanjiang Bay. The offset values are the measured values minus the theoretical mixed values, which are calculated using the conservative mixing model.

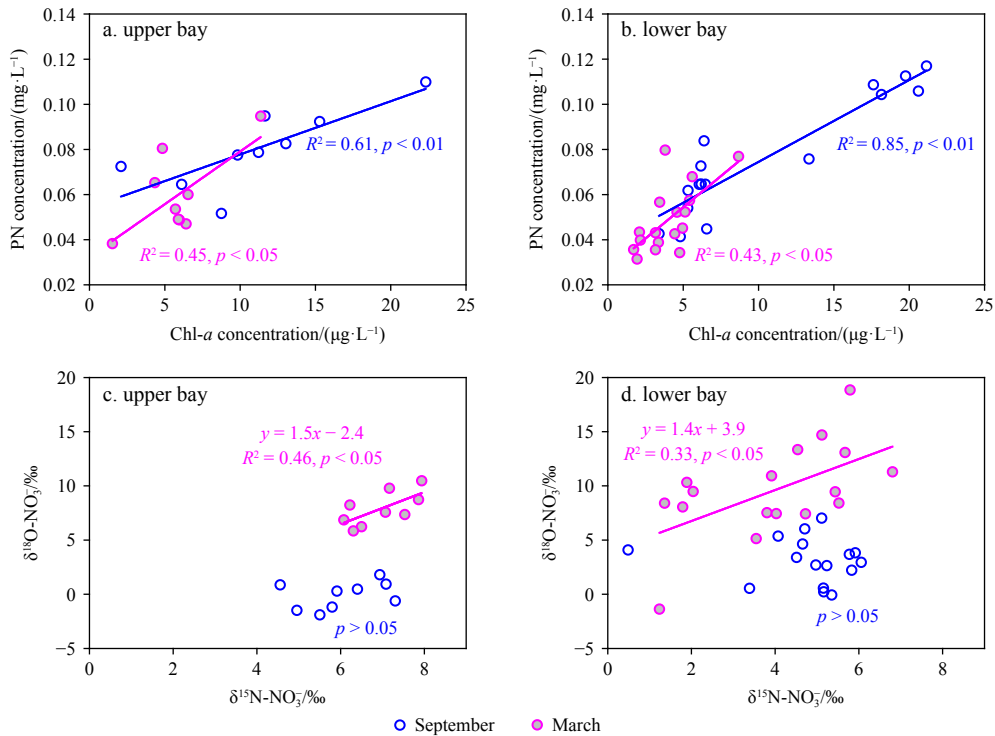


Fig. 6. Relation of PN concentration vs. Chl-*a* concentration, and $\delta^{15}\text{N-NO}_3^-$ vs. $\delta^{18}\text{O-NO}_3^-$ in the upper and lower bays during rainy and dry seasons.

the rainy season (Fig. 6), suggesting that phytoplankton biomass was the dominant component of PN. In addition, negative offset- $\delta^{15}\text{N-PN}$ values occurred in the lower bay during the rainy season (Fig. 5b), which could be influenced by the assimilation of NH_4^+ by phytoplankton due to the sufficient NH_4^+ (an average of

$5.04 \mu\text{mol/L}$). Sufficient NH_4^+ may be responsible for the higher Chl-*a* concentrations in both the upper and lower bays during the rainy season (Fig. 2g). Unlike the upper bay, the lower bay is broader and deeper owing to the influence of terrain and is thus less influenced by tidal pumping (Wang et al., 2021). Moreover,

the greater depth in the lower bay prevents exchange between the surface and bottom water because of strong stratification in the rainy season. This is supported by the higher temperature (an average of 31.39°C) and lower salinity (an average of 25.05) in the surface water, whereas the lower temperature (an average of 30.70°C) and higher salinity (an average of 26.74) in the bottom water.

In the dry season, a negative offset of NO_3^- was observed in both the upper and lower bays (Fig. 5a), indicating that removal of NO_3^- occurred within the bay. Different from the rainy season, extremely low NH_4^+ concentration ($<0.2 \mu\text{mol/L}$) (Fig. 3f) was observed in the bay, suggesting that NH_4^+ is almost completely consumed in the dry season. The overall positive offset $\delta^{15}\text{N}-\text{NO}_3^-$ and $\delta^{18}\text{O}-\text{NO}_3^-$ values (average of 1.5‰ and 3.5‰, respectively) and the significantly positive relation between them suggested that NO_3^- assimilation by phytoplankton occurred in the bay during this season. However, the slopes were >1 in both regions (Figs 6c and d), indicating that there may have been other processes or sources during this period. The significant positive correlations between Chl-*a* and PN in the two regions indicated that phytoplankton biomass was the major component of PN. However, unlike the rainy season, most offset $\delta^{15}\text{N}-\text{PN}$ values were above the mixing line (positive values) in the two regions during the dry season (Fig. 5b), suggesting the loss of PN (such as decomposition/mineralization) simultaneously occurred in the bay. This was consistent with the decrease in Chl-*a* concentration during the dry season (Fig. 2h). Interestingly, the offset $\delta^{15}\text{N}-\text{PN}$ values (-2.2‰ – -2.5‰) were within the range of offset $\delta^{15}\text{N}-\text{NO}_3^-$ values (-3.8‰ – -3.7‰) in the dry season, probably suggesting a strong coupling between assimilation and decomposition/mineralization (Ye et al., 2016).

Indeed, in mid-March 2018, a red tide of *Phaeocystis globosa* in Zhanjiang Bay, with a maximum cell density of 1.13×10^9 cells/L (2018 South China Sea Region Marine Disaster Bulletin; <http://scs.mnr.gov.cn/scsb/gbyjt/201911/b90b49d8b13e4f609ef31615fdde69c6.shtml>), occurred. The dry season, particularly late winter and early spring, is characterized by frequent algal blooms and red tides in Zhanjiang Bay (Zhang et al., 2022). The outbreak of red tides consumes large amounts of nutrients, especially ammonium. However, due to the sharp decrease in runoff during the dry season, the input of nutrients from terrestrial sources has significantly diminished (Lao et al., 2022b). The outbreak of red tides consumes a large amount of nutrients in the bay, resulting in decreased nutrients in the bay owing to the lack of external nutrient input during this period (He et al., 2023; Zhang et al., 2022). Owing to the high density of algae and insufficient nutrient supply for their continued growth, a large number of algae gradually began to die. The lower Chl-*a* concentration during the sampling period (at the end of March, during the late red tide period) is consistent with this phenomenon. Therefore, these algal deaths and gradual mineralization could contribute to elevating $\delta^{15}\text{N}-\text{PN}$ values in Zhanjiang Bay during the dry season.

Thus, the coupling between assimilation and decomposition/mineralization could be the dominant process in the bay during the dry season.

4.3 Quantification of nitrate sources in Zhanjiang Bay and its implications for marine eco-environment

Due to the reduced input of terrestrial nutrients and the dominance of biological processes (assimilation and mineralization) in isotopic fractionation, the isotopic values of nitrate cannot be used for source apportionment during the dry season. In contrast, despite some fluctuations, nitrate concentrations mainly aligned with the theoretical mixing line, indicating that nitrate was in a conservative mixing state during the rainy season, and that nitrate isotopes should be similar to the source. Therefore, we quantified the sources of nitrate in Zhanjiang Bay during the rainy season. Because Zhanjiang Bay is surrounded by cities and rivers, heavy rainfall can erode and wash away land-based pollutants from the basin into rivers, which then flow from the top of the bay to the lower bay during the rainy season. Thus, four potential nitrate sources, namely manure and sewage, fertilizer, soil N, and atmospheric deposition, were considered in this study. The values of $\delta^{15}\text{N}-\text{NO}_3^-$ and $\delta^{18}\text{O}-\text{NO}_3^-$ for the four potential nitrate sources are presented in Table 2. To quantify the proportional contributions of these nitrate sources, a Bayesian mixing model was used, and the results are shown in Fig. 7b. Soil N (36%) was the dominant nitrate source in Zhanjiang Bay during the rainy season, followed by manure and sewage (33%), and fertilizer (30%), while atmospheric deposition (only 1%) contributed less to the nitrate pool in the bay. These results were consistent with the findings from a classical nitrate dual isotopic approach depicted in Fig. 7. The $\delta^{15}\text{N}-\text{NO}_3^-$ and $\delta^{18}\text{O}-\text{NO}_3^-$ values in Zhanjiang Bay mainly fell in the sources of soil N and manure and sewage. Zhanjiang Bay experiences high rainfall and frequency during the rainy season (Chen et al., 2021). Rainwater erosion can transport a substantial amount of soil N from the basin into the bay, similar to findings in Qinzhou Bay, which shares similar climatic characteristics (Chen et al., 2022c). Moreover, many sewage outlets around Zhanjiang Bay directly discharge large amounts of urban and industrial wastewater into the bay (Chen et al., 2022b; He et al., 2023; Zhang et al., 2021). As shown in Fig. 7, the contribution of manure, sewage, and fertilizer to nitrate loads is very close to the contribution of soil N, suggesting that heavy rainfall in the rainy season can also input massive amounts of sewage and fertilizer N into Zhanjiang Bay. The elevated nutrient concentrations in Zhanjiang Bay during the rainy season may be attributed to abundant contaminants discharged from soil, sewage, and fertilizers. Due to intensive human activities, the intrusion of high-salinity water from the outer bay into the inner Zhanjiang Bay has significantly increased over the past two decades (Lao et al., 2022b). Particularly in the summer (rainy season), the stronger west-Guangdong coastal current in outer Zhanjiang Bay can increase high-salinity water intrusion (Lao et al., 2022b). In addition, Zhanjiang Bay is fre-

Table 2. The values (‰) of $\delta^{15}\text{N}-\text{NO}_3^-$ and $\delta^{18}\text{O}-\text{NO}_3^-$ for the four potential nitrate sources in Zhanjiang Bay

Source	$\delta^{15}\text{N}-\text{NO}_3^-$			$\delta^{18}\text{O}-\text{NO}_3^-$		
	Range/‰	(Mean \pm SD)/‰	Literature	Range/‰	(Mean \pm SD)/‰	Literature
Manure and Sewage	4 – 25	10.3 \pm 4.0	Xue et al., 2009	–5 – 15	4.08 \pm 0.33	Kendall, 1998; Zhang et al., 2018
Fertilizer	–1.87 – 2.96	0.04 \pm 1.87	Kendall, 1998; Zhang et al., 2018	–5 – 15	4.08 \pm 0.33	Kendall, 1998; Zhang et al., 2018
Soil N	–0.05 – 8.25	4.52 \pm 2.67	Kendall, 1998; Zhang et al., 2018	–5 – 15	4.08 \pm 0.33	Kendall, 1998; Zhang et al., 2018
Atmospheric N deposition	–1.8 – 4.1	0.8 \pm 1.5	Chen et al., 2019	42.7 – 61.6	52.4 \pm 5.1	Chen et al., 2019

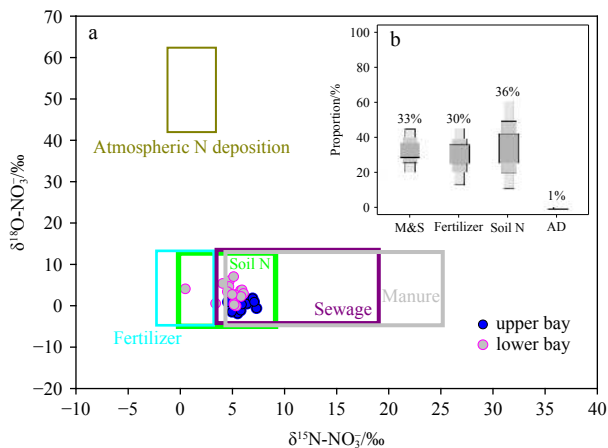


Fig. 7. Values of $\delta^{15}\text{N-NO}_3^-$ and $\delta^{18}\text{O-NO}_3^-$ in Zhanjiang Bay during the rainy season (a); the proportional contribution of potential nitrate sources in Zhanjiang Bay (b). The different colored boxes represent the range of isotopic values of potential sources of nitrate.

quently affected by typhoons, during which heavy rainfall can input large amounts of nutrients into Zhanjiang Bay (Lao et al., 2023c, 2023d; Zhou et al., 2021). However, typhoon storm surges can also intrude large amounts of high-salinity seawater into Zhanjiang Bay (Lao et al., 2023d). The mixing of high-salinity seawater intrusion and diluted freshwater in the bay forms a strong ocean front, thereby trapping a significant amount of pollutants within the bay (Lao et al., 2023d). This is also an important factor that exacerbates the eutrophication of seawater in Zhanjiang Bay (He et al., 2023), which must be considered by environmental managers.

5 Conclusions

Our study on the stable isotopes of particulate and dissolved N pools provides detailed insights into N sources and cycling in a typical mariculture bay. We observed significant seasonal variations in nutrient concentrations, with higher level in the rainy season and lower level in the dry season. This trend is primarily attributed to the influx of terrestrial nutrients discharged into the bay during the rainy season. In addition, significant nitrate loss occurred in the upper bay during the rainy season, which was related to intense physical sediment-water interactions, with less isotopic fractionation. Among the multiple sources, soil N (36%) and manure and sewage (33%) were the predominant N sources contributing to the N loads in Zhanjiang Bay during the rainy season. However, during the dry season, more biogeochemical processes in the bay may be related to a decrease in runoff and an increase in water retention time. Owing to the impact of red tides, the ammonium in Zhanjiang Bay has been almost completely consumed during the dry season. In addition, the observed nitrate loss and concurrent increase in stable isotopes of dissolved and particulate N during the dry season indicate strong coupling of assimilation and mineralization.

References

Chen Fajin, Deng Ziyun, Lao Qibin, et al. 2022a. Nitrogen cycling across a salinity gradient from the Pearl River Estuary to offshore: Insight from nitrate dual isotopes. *Journal of Geophysical Research: Biogeosciences*, 127(5): e2022JG006862, doi: [10.1029/2022JG006862](https://doi.org/10.1029/2022JG006862)

Chen Fajin, Huang Chao, Lao Qibin, et al. 2021. Typhoon control of

precipitation dual isotopes in southern China and its palaeoenvironmental implications. *Journal of Geophysical Research: Atmospheres*, 126(14): e2020JD034336, doi: [10.1029/2020JD034336](https://doi.org/10.1029/2020JD034336)

Chen Fajin, Lao Qibin, Jia Guodong, et al. 2019. Seasonal variations of nitrate dual isotopes in wet deposition in a tropical city in China. *Atmospheric Environment*, 196: 1–9, doi: [10.1016/j.atmosenv.2018.09.061](https://doi.org/10.1016/j.atmosenv.2018.09.061)

Chen Fajin, Lao Qibin, Liu Mengyang, et al. 2022b. Impact of intensive mariculture activities on microplastic pollution in a typical semi-enclosed bay: Zhanjiang Bay. *Marine Pollution Bulletin*, 176: 113402, doi: [10.1016/j.marpolbul.2022.113402](https://doi.org/10.1016/j.marpolbul.2022.113402)

Chen Chunqing, Lao Qibin, Shen Youli, et al. 2022c. Comparative study of nitrogen cycling between a bay with riverine input and a bay without riverine input, inferred from stable isotopes. *Frontiers in Marine Science*, 9: 885037, doi: [10.3389/fmars.2022.885037](https://doi.org/10.3389/fmars.2022.885037)

Chen Fajin, Lao Qibin, Zhang Shuwen, et al. 2020. Nitrate sources and biogeochemical processes identified using nitrogen and oxygen isotopes on the eastern coast of Hainan Island. *Continental Shelf Research*, 207: 104209, doi: [10.1016/j.csr.2020.104209](https://doi.org/10.1016/j.csr.2020.104209)

Dähnke K, Bahlmann E, Emeis K. 2008. A nitrate sink in estuaries? An assessment by means of stable nitrate isotopes in the Elbe Estuary. *Limnology and Oceanography*, 53(4): 1504–1511, doi: [10.4319/lo.2008.53.4.1504](https://doi.org/10.4319/lo.2008.53.4.1504)

Dai Minhan, Zhao Yangyang, Chai Fei, et al. 2023. Persistent eutrophication and hypoxia in the coastal ocean. *Cambridge Prisms: Coastal Futures*, 1: e19, doi: [10.1017/cft.2023.7](https://doi.org/10.1017/cft.2023.7)

Fry B. 2002. Conservative mixing of stable isotopes across estuarine salinity gradients: A conceptual framework for monitoring watershed influences on downstream fisheries production. *Estuaries*, 25(2): 264–271, doi: [10.1007/BF02691313](https://doi.org/10.1007/BF02691313)

Glibert P M, Wilkerson F P, Dugdale R C, et al. 2016. Pluses and minuses of ammonium and nitrate uptake and assimilation by phytoplankton and implications for productivity and community composition, with emphasis on nitrogen-enriched conditions. *Limnology and Oceanography*, 61(1): 165–197, doi: [10.1002/lno.10203](https://doi.org/10.1002/lno.10203)

Granger J, Sigman D M. 2009. Removal of nitrite with sulfamic acid for nitrate N and O isotope analysis with the denitrifier method. *Rapid Communications in Mass Spectrometry*, 23(23): 3753–3762, doi: [10.1002/rcm.4307](https://doi.org/10.1002/rcm.4307)

Granger J, Sigman D M, Lehmann M F, et al. 2008. Nitrogen and oxygen isotope fractionation during dissimilatory nitrate reduction by denitrifying bacteria. *Limnology and Oceanography*, 53(6): 2533–2545, doi: [10.4319/lo.2008.53.6.2533](https://doi.org/10.4319/lo.2008.53.6.2533)

He Guirong, Lao Qibin, Jin Guangzhe, et al. 2023. Increasing eutrophication driven by the increase of phosphate discharge in a subtropical bay in the past 30 years. *Frontiers in Marine Science*, 10: 1184421, doi: [10.3389/fmars.2023.1184421](https://doi.org/10.3389/fmars.2023.1184421)

Howarth R W. 2008. Coastal nitrogen pollution: a review of sources and trends globally and regionally. *Harmful Algae*, 8(1): 14–20, doi: [10.1016/j.hal.2008.08.015](https://doi.org/10.1016/j.hal.2008.08.015)

Kendall C. 1998. Tracing nitrogen sources and cycling in catchments. In: Kendall C, McDonnell J J, eds. *Isotope Tracers in Catchment Hydrology*. New York: Elsevier, 519–576

Khangaonkar T, Nugraha A, Xu Wenwei, et al. 2018. Analysis of hypoxia and sensitivity to nutrient pollution in Salish Sea. *Journal of Geophysical Research: Oceans*, 123(7): 4735–4761, doi: [10.1029/2017JC013650](https://doi.org/10.1029/2017JC013650)

Lao Qibin, Chen Fajin, Jin Guangzhe, et al. 2023a. Characteristics and mechanisms of typhoon-induced decomposition of organic matter and its implication for climate change. *Journal of Geophysical Research: Biogeosciences*, 128(6): e2023JG007518, doi: [10.1029/2023JG007518](https://doi.org/10.1029/2023JG007518)

Lao Qibin, Chen Fajin, Liu Guoqiang, et al. 2019. Isotopic evidence for the shift of nitrate sources and active biological transformation on the western coast of Guangdong Province, South China. *Marine Pollution Bulletin*, 142: 603–612, doi: [10.1016/j.marpolbul.2019.04.026](https://doi.org/10.1016/j.marpolbul.2019.04.026)

- Lao Qibin, Liu Sihai, Ling Zheng, et al. 2023b. External dynamic mechanisms controlling the periodic offshore blooms in Beibu Gulf. *Journal of Geophysical Research: Oceans*, 128(6): e2023JC019689, doi: [10.1029/2023JC019689](https://doi.org/10.1029/2023JC019689)
- Lao Qibin, Lu Xuan, Chen Fajin, et al. 2023c. Effects of upwelling and runoff on water mass mixing and nutrient supply induced by typhoons: Insight from dual water isotopes tracing. *Limnology and Oceanography*, 68(1): 284–295, doi: [10.1002/lno.12266](https://doi.org/10.1002/lno.12266)
- Lao Qibin, Lu Xuan, Chen Fajin, et al. 2023d. A comparative study on source of water masses and nutrient supply in Zhanjiang Bay during the normal summer, rainstorm, and typhoon periods: Insights from dual water isotopes. *Science of the Total Environment*, 903: 166853, doi: [10.1016/j.scitotenv.2023.166853](https://doi.org/10.1016/j.scitotenv.2023.166853)
- Lao Qibin, Wu Junhui, Chen Fajin, et al. 2022a. Increasing intrusion of high salinity water alters the mariculture activities in Zhanjiang Bay during the past two decades identified by dual water isotopes. *Journal of Environmental Management*, 320: 115815, doi: [10.1016/j.jenvman.2022.115815](https://doi.org/10.1016/j.jenvman.2022.115815)
- Lao Qibin, Zhang Shuwen, Li Zhiyang, et al. 2022b. Quantification of the seasonal intrusion of water masses and their impact on nutrients in the Beibu Gulf using dual water isotopes. *Journal of Geophysical Research: Oceans*, 127(7): e2021JC018065, doi: [10.1029/2021JC018065](https://doi.org/10.1029/2021JC018065)
- Li Jiacheng, Cao Ruixue, Lao Qibin, et al. 2020. Assessing seasonal nitrate contamination by nitrate dual isotopes in a monsoon-controlled bay with intensive human activities in South China. *International Journal of Environmental Research and Public Health*, 17(6): 1921, doi: [10.3390/ijerph17061921](https://doi.org/10.3390/ijerph17061921)
- McIlvin M R, Altabet M A. 2005. Chemical conversion of nitrate and nitrite to nitrous oxide for nitrogen and oxygen isotopic analysis in freshwater and seawater. *Analytical Chemistry*, 77(17): 5589–5595, doi: [10.1021/ac050528s](https://doi.org/10.1021/ac050528s)
- Sigman D M, Altabet M A, McCorkle D C, et al. 1999. The $\delta^{15}\text{N}$ of nitrate in the Southern Ocean: Consumption of nitrate in surface waters. *Global Biogeochemical Cycles*, 13(4): 1149–1166, doi: [10.1029/1999GB900038](https://doi.org/10.1029/1999GB900038)
- Sigman D M, Granger J, Difiore P J, et al. 2005. Coupled nitrogen and oxygen isotope measurements of nitrate along the eastern North Pacific margin. *Global Biogeochemical Cycles*, 19(4): GB4022
- Wang Shuangling, Zhou Fengxia, Chen Fajin, et al. 2021. Spatiotemporal distribution characteristics of nutrients in the drowned tidal inlet under the influence of tides: A case study of Zhanjiang Bay, China. *International Journal of Environmental Research and Public Health*, 18(4): 2089, doi: [10.3390/ijerph18042089](https://doi.org/10.3390/ijerph18042089)
- Wankel S D, Kendall C, Pennington J T, et al. 2007. Nitrification in the euphotic zone as evidenced by nitrate dual isotopic composition: Observations from Monterey Bay, California. *Global Biogeochemical Cycles*, 21(2): GB2009
- Xue Dongmei, Botte J, De Baets B, et al. 2009. Present limitations and future prospects of stable isotope methods for nitrate source identification in surface- and groundwater. *Water Research*, 43(5): 1159–1170, doi: [10.1016/j.watres.2008.12.048](https://doi.org/10.1016/j.watres.2008.12.048)
- Yan Xiuli, Xu M N, Wan X S, et al. 2017. Dual isotope measurements reveal zoning of nitrate processing in the summer Changjiang (Yangtze) River plume. *Geophysical Research Letters*, 44(24): 12289–12297
- Yang Zhi, Chen Jianfang, Li Hongliang, et al. 2018. Sources of nitrate in Xiangshan Bay (China), as identified using nitrogen and oxygen isotopes. *Estuarine, Coastal and Shelf Science*, 207: 109–118
- Ye Feng, Jia Guodong, Xie Luhua, et al. 2016. Isotope constraints on seasonal dynamics of dissolved and particulate N in the Pearl River Estuary, South China. *Journal of Geophysical Research: Oceans*, 121(12): 8689–8705
- Zhang Peng, Peng Conghui, Zhang Jibiao, et al. 2022. Long-term harmful algal blooms and nutrients patterns affected by climate change and anthropogenic pressures in the Zhanjiang Bay, China. *Frontiers in Marine Science*, 9: 849819, doi: [10.3389/fmars.2022.849819](https://doi.org/10.3389/fmars.2022.849819)
- Zhang Jibiao, Zhang Yanchan, Zhang Peng, et al. 2021. Seasonal phosphorus variation in coastal water affected by the land-based sources input in the eutrophic Zhanjiang Bay, China. *Estuarine, Coastal and Shelf Science*, 252: 107277
- Zhang Man, Zhi Yuyou, Shi Jiachun, et al. 2018. Apportionment and uncertainty analysis of nitrate sources based on the dual isotope approach and a Bayesian isotope mixing model at the watershed scale. *Science of the Total Environment*, 639: 1175–1187, doi: [10.1016/j.scitotenv.2018.05.239](https://doi.org/10.1016/j.scitotenv.2018.05.239)